Impulsive solvent heating probed by picosecond x-ray diffraction

M. Cammarata
European Synchrotron Radiation Facility, BP 220, Grenoble Cedex 38043, France; National Institute for the Physics of Matter, 16152 Genova, Italy; and Department of Physical and Astronomical Sciences, via Archirafi 36, Palermo, Italy

M. Lorenc[a)]
European Synchrotron Radiation Facility, BP 220, Grenoble Cedex 38043, France

T. K. Kim and J. H. Lee
Department of Chemistry, Korea Advanced Institute of Science and Technology (KAIST), Daejeon 305-701, Republic of Korea and School of Molecular Science (BK21), Korea Advanced Institute of Science and Technology (KAIST), Daejeon 305-701, Republic of Korea

Q. Y. Kong
European Synchrotron Radiation Facility, BP 220, Grenoble Cedex 38043, France

E. Pontecorvo
Dipartimento di Fisica, Università di Roma "La Sapienza," I-00185 Roma, Italy and SOFT-INFM-CNR, Università di Roma "La Sapienza," I-00185 Roma, Italy

M. Lo Russo
European Synchrotron Radiation Facility, BP 220, Grenoble Cedex 38043, France

G. Schiró and A. Cupane
National Institute for the Physics of Matter, 16152 Genova, Italy and Department of Physical and Astronomical Sciences, via Archirafi 36, Palermo, Italy

M. Wulff
European Synchrotron Radiation Facility, BP 220, Grenoble Cedex 38043, France

H. Ihee[b)]
Department of Chemistry, Korea Advanced Institute of Science and Technology (KAIST), Daejeon 305-701, Republic of Korea and School of Molecular Science (BK21), Korea Advanced Institute of Science and Technology (KAIST), Daejeon 305-701, Republic of Korea

(Received 14 November 2005; accepted 17 January 2006; published online 23 March 2006)

The time-resolved diffraction signal from a laser-excited solution has three principal components: the solute-only term, the solute-solvent cross term, and the solvent-only term. The last term is very sensitive to the thermodynamic state of the bulk solvent, which may change during a chemical reaction due to energy transfer from light-absorbing solute molecules to the surrounding solvent molecules and the following relaxation to equilibrium with the environment around the scattering volume. The volume expansion coefficient α for a liquid is typically $\sim 1 \times 10^{-3}$ K^{-1}, which is about 1000 times greater than for a solid. Hence solvent scattering is a very sensitive on-line thermometer. The decomposition of the scattered x-ray signal has so far been aided by molecular dynamics (MD) simulations, a method capable of simulating the solvent response as well as the solute term and solute/solvent cross terms for the data analysis. Here we present an experimental procedure, applicable to most hydrogen containing solvents, that directly measures the solvent response to a transient temperature rise. The overtone modes of OH stretching and CH_3 asymmetric stretching in liquid methanol were excited by near-infrared femtosecond laser pulses at 1.5 and 1.7 μm and the ensuing hydrodynamics, induced by the transfer of heat from a subset of excited CH_3OH^* to the bulk and the subsequent thermal expansion, were probed by 100 ps x-ray pulses from a synchrotron. The time-resolved data allowed us to extract two key differentials: the change in the solvent diffraction from a temperature change at constant density, seen at a very short time delay $\sim$100 ps, and a term from a change in density at constant temperature. The latter term becomes relevant at

[a)]Present address: Groupe Matiere Condensee et Materiaux UMR6626 CNRS, BAT11A Campus de Beaulieu, Universite de Rennes 1, 35042 Rennes Cedex, France.
[b)]Author to whom correspondence should be addressed. Electronic mail: hyotcherl.ihee@kaist.ac.kr

later times ~1 μs when the bulk of liquid expands to accommodate its new temperature at ambient pressure. These two terms are the principal building blocks in the hydrodynamic equation of state, and they are needed in a self-consistent reconstruction of the solvent response during a chemical reaction. We compare the experimental solvent terms with those from MD simulations. The use of experimentally determined solvent differentials greatly improved the quality of global fits when applied to the time-resolved data for $C_2H_4I_2$ dissolved in methanol. © *2006 American Institute of Physics*. [DOI: 10.1063/1.2176617]

I. INTRODUCTION

Solution-phase chemistry is a very important field of research since the majority of life processes and industrial processes take place in solution.[1] Studying this environment with x rays is ideal since x rays can penetrate bulk samples and hence reveal the elementary principles driving chemical reactions. Recent years have witnessed great advances in time-resolved x-ray diffraction (TRXD) from laser-excited molecules in liquids.[2–6] Technological innovations[4,7] in synchrotron instrumentation and the development of novel data analysis[6] have made it possible to track complex reactions in solution by time-resolved diffraction to temporal and spatial resolutions of 100 ps and 0.001 Å, respectively. For instance, the photodissociation reaction of $C_2H_4I_2$ in methanol was recently investigated by this technique and the data analysis revealed a rather complex reaction pathway comprising a bridged C_2H_4I radical, a linear isomer C_2H_4I–I, and the end product C_2H_4+I_2.[6] Moreover with TRXD, the properties and structures of elemental liquids can be studied too.[6,8]

Compared with the gas phase, the solution phase is experimentally more challenging due to the presence of a large number of solvent molecules around the solute molecule of interest. Whereas the diffraction signal in the gas phase comes only from isolated (noninteracting) molecules (solutes),[9] the diffraction signal in solution is the (incoherent) sum of the solute-only term, the solute-solvent cross term, and the solvent-only term. The last term is related to the change in the diffraction intensity caused by temperature and density changes in the bulk solvent, which are caused by energy transfer from the light-absorbing solute molecule to surrounding solvent molecules. Due to this complexity, fingerprinting of the molecules in action would not be possible were it not aided by the theory. Molecular dynamics (MD) simulation can simulate statistical atom-atom correlation functions $g_{\alpha\beta}(r)$ for a solution.[10,11] These simulations are indispensable for disentangling the different contributions in the scattering patterns, and they have proved quite accurate in reproducing measured signals. However, numerous factors influence the accuracy of these simulations. First of all, theoretical potentials define trajectories on which molecules evolve; hence the structure determination may depend on the type of potential used. Certain force fields are difficult to model efficiently: the most well-known example is the force field associated with hydrogen bonds (methanol, water, etc.). The simulations are run on a finite ensemble of molecules, which define the simulation box size, thus putting a constraint on the lowest q and on the real space analysis. For these reasons, it is desirable to obtain the solvent-only term experimentally. Armed with experimental solvent differentials, one can, in principle, subtract the solvent contribution and deduce the structure of the caged solutes during the reaction.

We noticed recently that these terms, in many solvents, can be measured directly and here we report on a direct determination of the experimental solvent differentials by time-resolved x-ray diffraction on a pure solvent (methanol) heated by 100 fs pulses of near-infrared (IR) radiation. The key idea is that the near-IR pulses excite overtones of O–H and CH_3 vibrations in liquid methanol, and in doing so, they deposit heat without inducing any chemical change. It can be shown that for neat liquids, the time needed to reach a uniform temperature in a typical experiment is smaller than 100 ps (see later). This fact justifies the use of hydrodynamics equations for time delays larger than 100 ps; these equations show that at early time delays, the volume and the density of the solvent do not change, and consequently only the effective temperature (and pressure) of the solvent rises.[12] The laser-induced change is obtained by subtracting the nonexcited scattering, measured at a negative time delay, from the scattering at a very short time delay ~100 ps. This gives the change in the diffraction intensity due to a temperature change at constant density, $(\partial S/\partial T)_\rho$, where S stands for the diffraction intensity, T the temperature, and ρ the density.[10] At later time delays, pressure relaxation, being faster than the thermal one, drives the system into a configuration of a hot solvent at ambient pressure, i.e., thermal expansion. The difference between the diffracted intensity at a late time delay yields the constant pressure term, $(\partial S/\partial T)_P$, where P stands for the pressure. By combining the two terms $[(\partial S/\partial T)_\rho$ and $(\partial S/\partial T)_P]$, one can get the principal differentials $(\partial S/\partial T)_\rho$ and $(\partial S/\partial \rho)_T$ (see later).

Subsequently, these experimental methanol differentials were applied to our analysis of the dissociation of $C_2H_4I_2$ in methanol. Compared to our previous fits with MD solvent differentials, the new fits noticeably improve the comparison between experiment and theory, especially at low q in q space and everywhere in r space.

We explain the experimental details in Sec. II. In Sec. III, we present the steps in the data reduction and discuss how to obtain the experimental differentials. The fits with the old (MD) components and with new experimental components are also compared in Sec. III.

II. EXPERIMENT

The tunable femtosecond laser on beamline ID09B at the European Synchrotron Radiation Facility (ESRF) was used to generate 100 fs near-IR (NIR) radiation. The system is based on a Ti:sapphire oscillator (MIRA from Coherent), the output of which was amplified in a chirped pulse amplifier

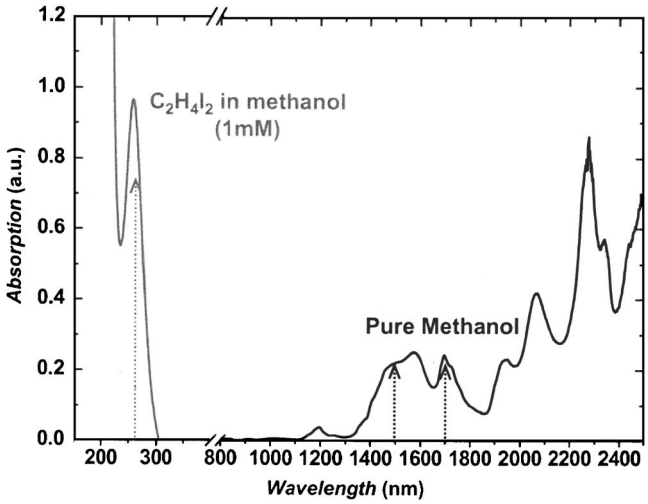

FIG. 1. Absorption spectrum of $C_2H_4I_2$ dissolved in methanol (1 mM) in the range from UV to NIR. The optical density for the solute at 267 nm is comparable to that for the solvent at 1500 and 1700 nm.

(CPA), the Hurricane from Spectra Physics, operating at a frequency of 986.2 Hz, and the 360th subharmonic of the orbit frequency of an electron bunch in the synchrotron. The 800 nm output from the Hurricane seeds an optical parametric amplifier, the Topas from Light Conversion, in which it is down converted into two NIR pulses: the 1500 nm (signal) and the 1700 nm (idler). The signal at 1500 nm corresponds to the first overtone of OH stretching whose fundamental is at $\sim 3337\ \mathrm{cm}^{-1}$ and the idler at 1700 nm to the first overtone of the CH_3 asymmetric stretching mode whose fundamental is at $\sim 2934\ \mathrm{cm}^{-1}$.[13] The pulse duration is estimated to be 100 fs, and the total generated infrared energy was 100 μJ at the sample. The signal and idler were cross polarized with each in a power ratio of 1:1. The beams were focused to a 100 μm diameter spot [full width at half maximum (FWHM)]. The estimated absorbed heat ($\sim 9\ \mu$J/pulse) due to the infrared absorption in methanol is comparable to that released to methanol during the chemical reactions we have studied so far (10–20 μJ/pulse) in TRXD experiments.[2,5,6] As an example, the absorption spectrum of a 1 mM solution of $C_2H_4I_2$ in methanol is shown in Fig. 1 over the range from UV to near IR. It is clear that the optical density for the solute at 267 nm is comparable to that for the solvent at 1500 and 1700 nm.

Polychromatic x-ray pulses of ~ 100 ps duration and $\sim 5\times 10^8$ photons per pulse were delivered by the U17 in-vacuum undulator. The x-ray spectrum was peaked at 18.2 keV and had a bandwidth of 0.45 keV (2.5% bandwidth). A high-speed chopper (Julich) spinning at the same frequency as the laser was used to select single pulses of x rays from the 16-bunch mode at the ESRF, where the x-ray pulses are separated by 176 ns. The x-ray beam was focused by a toroidal mirror to a spot size of $0.1\times 0.05\ \mathrm{mm}^2$ at the sample. The scattered x-ray signal was recorded on a 133 mm diameter fiber-coupled MarCCD at well defined time delays relative to the excitation pulse. The time delay between the two pulses was controlled electronically to an accuracy limited by electronic jitter, less than 3 ps (rms). At longer times, however, the decay in the bunch charge circulating in the synchrotron ring led to a systematic shift, which was measured to change by about −1.5 ps for a decay in synchrotron current of 10 mA. As the current in 16-bunch mode decays from 90 to 60 mA during a fill, the bunch arrives 4.5 ps earlier at the end of a fill, which is negligible compared to the 100 ps pulse length.

Concerning the sample cell system, two different setups were used: a capillary-based system and an open-jet one. In the first system, methanol was circulated through a quartz capillary (0.3 mm diameter) to provide a stable flow. In the open-jet system, the capillary was removed and a stable jet was produced by a high-pressure slit nozzle (slit, 0.3 mm, Kyburz) at a speed ensuring the refreshment of probe volume for every laser pulse. The open-jet system has the advantage over the capillary system that the scattering from the capillary materials is absent, which reduces the background substantially and increases the signal to noise ratio. The lower background also increases the accuracy of the normalization process (this is discussed in Secs. III C and III D). The sample was purchased from Merck and used without further purification. Time-resolved data on $C_2H_4I_2$ dissolved in methanol were taken from previous experiments[6] and reanalyzed.

Since the $(\partial S/\partial T)_P$ term for pure methanol is necessary for a proper absolute scaling of the experimental differentials obtained from the NIR experiment, a series of separate measurements were conducted on pure methanol as follows. A monochromatic x-ray beam at 26 keV was sent through liquid methanol contained in a sample cell designed for stable temperature control. The diffraction data were taken at four different temperatures: 15.0, 17.5, 20.0, and 22.5 °C.

III. RESULTS AND DISCUSSION

A. Data collection

The data were collected by exposing the charge-coupled device (CCD) for 12 s and, given the 1 kHz repetition rate of the laser/x-ray beam, the camera received 12 000 x-ray pulses per image. The pixels in a single image received between 3500 and 25 000 photons (for the maximum scattering angle and the liquid peak, respectively). The images were collected in pairs, with and without laser, for all time delays. This data collection cycle was repeated 100 times, which typically took 4.5 h.

After collection the images were radially integrated using FIT2D.[14] The one dimensional radial curves were then corrected for absorption in the phosphor screen in the CCD (conversion of x-ray photons to visible light photons). Without this correction, the signal amplitudes at high angles would have been artificially strong; the x rays are more efficiently converted to signal at high angles as the optical path in the phosphor scales as $1/\cos(2\theta)$ for a flat screen, where 2θ is the scattering angle. Due to the low absorption of methanol at 18 keV, no correction for the angular dependent x-ray absorption was made.

B. Normalization of the diffraction patterns

The laser-induced changes are small ($\Delta S/S < 0.2\%$) and in order to visualize them, the experimental data are pre-

sented as radial difference curves, generated by subtracting laser-on from laser-off images. Given the weak laser-induced change in the total scattering, the images are subject to judicious normalization prior to subtraction. Firstly, we scale the exposure time to compensate for the decrease in intensity of the incoming x-ray beam, due to the decaying bunch charge of the electrons circulating in the synchrotron ring. This ensures that equivalent images are exposed to the same level, which reduces the effect from nonlinear response in the CCD detector. Secondly, the fast transfer of heat from excited molecules to the bulk forces the solution to expand. The expansion takes place on a time scale determined by the time it takes sound waves to traverse the laser illuminated volume. In fast reactions and with current beam sizes $\sim 100\ \mu$m, the expansion happens between 10 and 100 ns.[10] This means that the number of molecules is generally different in laser-off and laser-on images. To correct for these effects, we use the recorded image itself as a monitor of the incoming x-ray intensity and the density of scattering centers (atoms). Specifically, we use a small interval around an isobestic point q_0 in the high-q part of the spectrum as the normalization range. The radial intensity is then divided by the integral count in this interval. The definition of an isobestic point is that the intensity at that particular q value is constant regardless of time delay. An initial candidate q_0 can be located from theoretical difference curves and further refined using a simple iterative procedure. Starting with a relatively broad interval around the initial q_0 ($q_0 > 7$ Å^{-1}, $\Delta q \sim 1.5$ Å^{-1}), the procedure checks for nodal points in the difference curves in the chosen range around q_0; the procedure is reiterated by changing the central point q_0 until the nodal point q_0 is well defined, i.e., until q_0 becomes an isobestic point. Usually, after two to three repetitions q_0 converges to a value within 0.02 Å^{-1} spread, and it becomes insensitive to the normalization interval (typical value used ~ 0.6 Å^{-1}). Changing q_0 by 0.02–0.05 Å^{-1} around the optimal value does not change the difference maps appreciably. In the reported experiment no significant dependence of q_0 with the time delay has been noticed.

C. Subtraction routine and generating difference maps

After having normalized the radial curves, the associated curves are subtracted to give difference curves. Due to the presence of background scattering, i.e., air and capillary when used, direct subtraction introduces spurious effects. In fact, with the density of the solution being time dependent [i.e., for time delays beyond 10 ns (Refs. 5 and 11)], the ratio of scattered intensity from the sample and the background becomes time dependent. In a typical experiment, the relative density change is $\sim 0.3\%$. This effect is readily corrected under the assumption that the total scattering is a sum of sample and background scattering and that the density change is known. The first assumption implies that the background scattering can be measured reliably by simply removing the sample (leaving the empty capillary, when used). As far as the density change is concerned, an iterative procedure will provide the right value as follows. In the first step, this correction is neglected and $\Delta\rho$ is estimated using the real

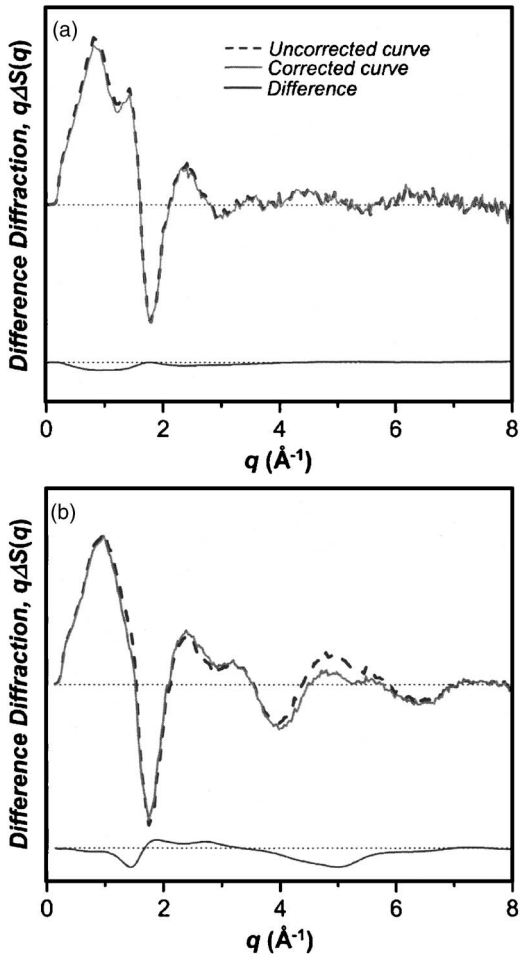

FIG. 2. Effect of the correction for the transient expansion of the liquid. Panel (A): pure methanol at 1 μs time delay with an open-jet system. Panel (B): $C_2H_4I_2$/methanol for 1 μs time delay. The broken lines are uncorrected curves and the solid lines corrected ones. The differences are also shown.

space Fourier transform of the data, scaled to absolute units (see below), in the $r \to 0$ limit.[10] This $\Delta\rho$ is an initial value in Eq. (1), the output of which generates a corrected difference curve ΔS_S (derivation in Appendix A):

$$\Delta S_S = \frac{1+\alpha/\beta}{1+\alpha}\left\{\Delta S_M + \frac{1-\beta}{\beta+\alpha}[\alpha S^{\text{off}}_{\text{sample}} - S_{\text{back}}]\right\}, \qquad (1)$$

where α is the fractional intensity from the background at q_0, $\beta = 1 + \Delta\rho/\rho$, ΔS_M is the uncorrected difference curve, $S^{\text{off}}_{\text{sample}}$ is the scattering intensity of the solution alone without laser, and S_{back} is the background scattering. Three or four reiterations of the procedure are enough to yield a satisfactory result. Figure 2 shows the effect of the correction for the time-resolved data on pure methanol and $C_2H_4I_2$/methanol at the time delay of 1 μs. At 100 ps, the density change is negligible, and therefore the corrected one equals to the uncorrected signal (not shown). However, a significant improvement is evident for 1 μs, where the density change was significant. The correction factor for the $C_2H_4I_2$/methanol data is higher than that of pure methanol because the density change in the former is larger.

To our knowledge, this correction for the laser-induced density change has not yet been discussed in the context of pump-probe experiments in general. This is probably be-

cause in the vast majority of optical pump-probe measurements the investigated time delays are at most within a few nanoseconds from time zero where the thermal expansion is not active yet and the solute concentrations are very small (micromolar), thereby $\Delta\rho/\rho$ being minute, of the order of $10^{-5}-10^{-4}$. This estimation is based on the formula (derivation in Appendix B)

$$\frac{\Delta\rho}{\rho} = \alpha_P \frac{fh\nu}{C_p}, \tag{2}$$

where α_P is the (volume) expansion coefficient at constant pressure, f is the fraction of photon absorbing molecules in the solution, h is Planck's constant, ν is the frequency of the optical pump, and C_P is the specific heat per molecule.

The real space difference maps are obtained by Fourier transforming the data. The detailed description can be found in a previous publication.[6] The nature of the difference maps in the TRXD measurements is such that a weak photoinduced signal has to be extracted from a large background. To obtain reliable difference maps various routines were tried, and the merit of each was checked against the reproducibility of difference maps. This can be quantified by considering the standard deviation for every q data point collected. The collection of laser-off and laser-on images, alternately, served to eliminate possible drifts in the experiment (temperature of the solution, beamline, etc.). Moreover, we found that the best results are obtained by using as the laser-off image the average between two such laser-off images recorded before and after the recording of a given laser-on image. Averaging 10–100 difference maps per time delay gives a good estimation of the error bars for every q, from the standard deviation from the mean value. The error bars thus obtained account only for statistical noise and not systematic errors. Very often the result in reciprocal space is not intuitive, and for this reason the experimental result is transformed to real space where the changes are more readily interpretable. An inherent drawback of this approach is that the Fourier transform acts as a "high frequency filter," thus artificially smoothes out the noise from photon statistics in q space. Yet, it is essential to estimate the error bars in real space. We propose the same procedure as the one just described for the q-space data: taking the Fourier transform (FT) of every single difference map and then averaging all the maps, which defines a meaningful standard deviation.

D. Methanol hydrodynamics

In this section we describe the theory-founding features of the temporal behavior of the solvent when impulsively heated with NIR radiation. In general, the temporal evolution of the solvent response can be described as a linear combination of two components pertaining to the photoinduced change in two independent thermodynamical parameters, arbitrarily chosen amongst density, temperature, and pressure. In Fig. 3 we show the methanol response measured for three time delays. It can be shown by solving the hydrodynamic equations[15] that for time delays sufficiently short $t < \tau_L = L/c$, where τ_L is the so-called Longaker-Litvak time, L is laser beam size and c the speed of sound in the liquid, the solvent is heated at constant volume. In the present experiment, $c = 1143$ m/s and $L \sim 50$ μm, which leads to $\tau_L \sim 44$ ns. On longer time scales, 10–100 ns, the pressure relaxes, causing expansion of the solvent. The solvent, at any time, can be fully described by two hydrodynamic variables (for example, temperature T and density ρ):

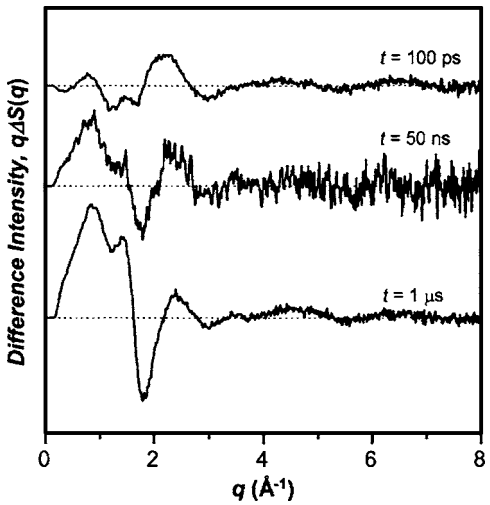

FIG. 3. Transient heating of methanol resolved in q as a function of time for selected time delays. Data at 100 ps and 1 μs were collected with a higher number of repetitions.

$$\Delta S(t) = \left(\frac{\partial S}{\partial T}\right)_\rho \Delta T(t) + \left(\frac{\partial S}{\partial \rho}\right)_T \Delta\rho(t). \tag{3}$$

The presence of only two components in the solvent response has been verified using the singular value decomposition (SVD) method,[16] which showed only two significant singular vectors. The SVD analysis showed unequivocally the reliability of the data and the data reduction routines. The NIR experiment on the pure solvent has the advantage over the UV-visible experiment that it does not generate any photochemistry on times relevant to the temporal resolution of the TRXD technique ($\sim$100 ps). After extremely fast vibrational cooling of methanol, well below 10 ps, the response of the solvent is entirely due to hydrodynamics. Therefore, it is relatively easy to determine the derivatives in Eq. (3), by measuring the response at two time delays only. For this reason we collected, with greatly enhanced statistics, diffraction patters at 100 ps and 1 μs. The 100 ps data are essentially $(\partial S/\partial T)_\rho$ multiplied by the temperature rise at this early stage of heating at constant volume, hence the second term contributing net zero. At 1 μs the liquid returns to ambient pressure. Therefore, the 1 μs data equal $(\partial S/\partial T)_P$ multiplied by the temperature rise at 1 μs. As shown in Fig. 4(a), the temperature rise at 1 μs was estimated to be 1.50 K by scaling the 1 μs data to $(\partial S/\partial T)_P$ determined experimentally from a series of static measurements at various temperatures. At 1 μs, the solvent is still hot, yet its temperature has lowered from the temperature at 100 ps by the ratio C_V/C_P due to expansion. Therefore, the temperature rise at 100 ps is 1.76 K and the experimental $(\partial S/\partial T)_\rho$ can be obtained by dividing 100 ps data by this number. $\Delta\rho$ at 1 μs can be calculated to be -1.77 kg/m^3 from the known isobaric thermal expansion coefficient of 1.49×10^{-3} K^{-1}. The equation of

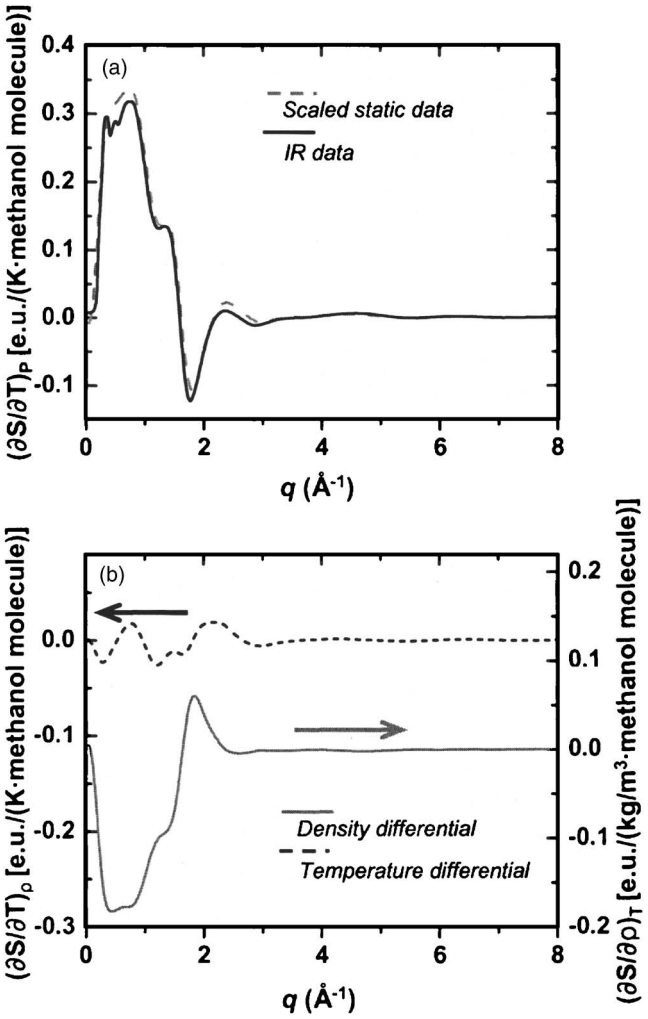

FIG. 4. Derivatives from the hydrodynamic equation of state for methanol. Panel (A): a comparison of the 1 μs data (solid) multiplied by 1.5 K with $(\partial S/\partial T)_P$ (broken) determined experimentally from a series of static measurements at various temperatures. Panel (B): two principal solvent differentials $(\partial S/\partial T)_\rho$ (broken) and $(\partial S/\partial \rho)_T$ (solid) obtained in this work (see text).

state [Eq. (3)] for the liquid at 1 μs can be rewritten as

$$\left(\frac{\partial S}{\partial \rho}\right)_T \Delta\rho = \Delta S(1\,\mu s) - \frac{C_V}{C_P}\Delta S(100\text{ ps}). \tag{4}$$

Then the experimental $(\partial S/\partial \rho)_T$ is obtained from Eq. (4). Figure 4(b) shows the experimental derivatives for methanol obtained through these procedures.

The concentration of the methanol molecules that absorb the NIR and contribute to the heating was estimated to 40 mM by considering the temperature change. As the concentration of pure methanol at ambient conditions is 24.7 M, this corresponds to exciting 1 out of 618 molecules. The total energy deposited to the irradiated volume is estimated to be $\sim$9 μJ/pulse by considering the total volume exposed to the NIR laser pulse.

The validity of classical hydrodynamics assumes a homogeneous and isotropic sample, thus it is important to estimate the time it takes to smooth out the memory of time zero, which can be described as a collection of hot points in the liquid. To estimate this thermalization time, we note that

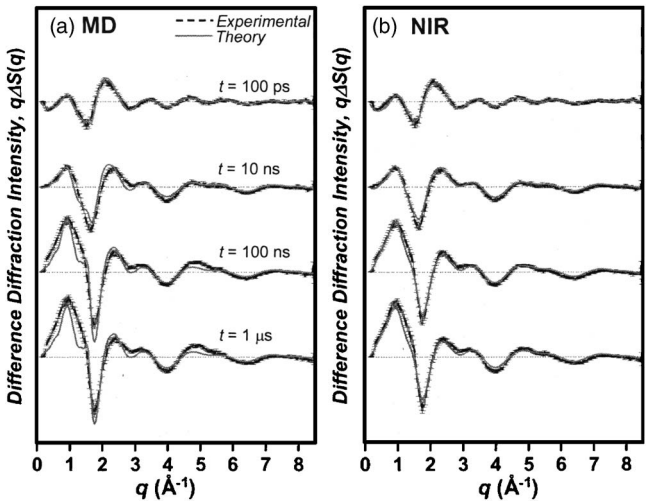

FIG. 5. Time-resolved diffraction signal as a function of time delay for $C_2H_4I_2$ in methanol at a few selected time delays; difference maps in q space. Panel (A): global fitting of all reaction components (solid) to experimental data (broken); the solvent components taken from MD simulation. Panel (B): like (A), but the solvent components are experimentally obtained from pure methanol excited by NIR pulses. The improvement is clear at low q for data at time delays beyond 30 ns.

the average distance between excited methanol molecules, at the observed 40 mM concentration, is 21.5 Å if the volume per excited solute is approximated by a sphere. Following the classical thermal diffusion theory developed by Landau and Lifshitz, a hot point in a liquid cools down in time and space following the equation

$$T(r,t) \propto \frac{1}{8(\pi\chi t)} \exp(-r^2/(4\chi t)), \tag{5}$$

with

$$\chi = \frac{\kappa}{\rho C_V}. \tag{6}$$

Here χ is the thermometric conductivity and κ the thermal conductivity. Note that the space dependence is contained in the exponential and that the position of the midpoint in the space distribution moves as

$$r_{50\%}(t) = 2\ln 2\sqrt{\chi t}. \tag{7}$$

The parameters for methanol are ρ=791 kg/m^3, C_V =2151 J/K/kg, κ=0.21 J/s/m/K, and χ=1.2345 $\times 10^{-7}$ m^2/s. From Eq. (7), we deduce that it takes 13.5 ps, on average, for two neighboring spherical thermal waves to meet, which is the criteria for local thermal homogeneity. As the scattering data presented here are ensemble averaged by our 100 ps long x-ray pulse, it is justified to use classical hydrodynamics in this work. In future experiments with pulsed x-ray lasers (XFEL) with 100 fs x-ray pulses, the earliest time delays will show the signature from the cooling of hot points.

E. Application of experimental solvent differentials

The experimental solvent differentials were applied to the time-resolved data on $C_2H_4I_2$ dissolved in methanol.[6] In Figs. 5 and 6 we demonstrate the extent to which the data

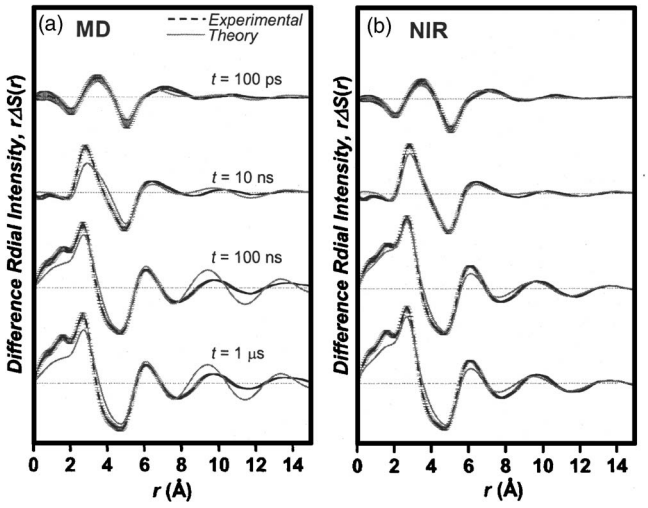

FIG. 6. Real space representation of the curves in Fig. 5. The improvement is clear for entire r for data at time delays beyond 30 ns.

analysis of a complex chemical reaction in methanol solution can be improved by applying the measured solvent response. As expected, the most pronounced effect of experimentally resolved hydrodynamics is seen at low q for data at late time delays after 30 ns, as shown in Fig. 5. This discrepancy is present over the entire r range in Fig. 6, where the improvement is more striking. The total χ^2 of the least-squares fit is reduced by 30% when MD solvent terms are replaced with the experimental ones. The fit parameters of the global analysis are compared in Table I. We note that the overall kinetics and conclusions regarding the structural dynamics have not changed although the quality of the fits is significantly improved. Since we used the experimental differentials obtained from the NIR experiment as the solvent response terms, it is important to scale these terms correctly. To see the effect of wrong scaling, we have fitted our data with the solvent terms with incorrect scaling. It turned out that a wrong scaling affects only the fraction of the rapidly cooled molecules, which again affect the magnitude of the final temperature rise and density drop. The overall kinetics was not affected. The time-dependent changes in the solute concentration, solvent density, and solvent temperature are shown in Fig. 7. The total energy deposited to the solution by a laser pulse is estimated to be ~ 12 μJ/pulse by considering the concentration of the excited molecules and the volume irradiated by the laser pulse. The improved fits add higher fidelity to our previous conclusions on the complex reaction pathway consisting of a bridged C_2H_4I radical, a C_2H_4I–I isomer, and finally $C_2H_4+I_2$ products.[6]

IV. CONCLUSIONS

We have demonstrated the use of time-resolved x-ray diffraction to study transient heating and the ensuing hydrodynamics of a common solvent. NIR femtosecond pulses were used to excite the overtones of OH stretching and CH_3 asymmetric stretching modes in liquid methanol, and picosecond x-ray pulses from a synchrotron were utilized to probe the heat-induced dynamics of methanol. Time-resolved data on pure methanol excited by infrared light allowed us to derive the responsive change in the diffracted intensity from the solvent due to a temperature change at constant density and due to a density change at constant temperature. These two terms are the hydrodynamic building blocks for global analysis of excited solutes dissolved in methanol. The use of these experimentally determined solvent differential terms greatly improved the quality of global fits when applied to the time-resolved data for $C_2H_4I_2$ in methanol. The experimental technique has now matured to tackle relatively complex chemical reactions in solution and now opens new possibilities for selective studies of either solvent hydrodynamics or chemistry of photoactive molecules. The ability to discriminate between different reaction channels is greatly enhanced by treating the solvent response with experimental solvent differentials.

TABLE I. Comparison of the global fit results using MD solvent differentials and experimental solvent differentials.

	MD solvent differentials	Experimental solvent differentials
Fractional concentration of excited molecules[a]	0.138 $(\pm 1.3\times 10^{-2})$[b]	0.162 $(\pm 1.3\times 10^{-3})$[b]
Fractional concentration of rapidly cooled molecules[a]	0.083 $(\pm 1.2\times 10^{-2})$[b]	0.106 $(\pm 1.3\times 10^{-2})$[b]
Fraction of rapidly cooled molecules[c]	0.60	0.65
$C_2H_4I_2\rightarrow C_2H_4I+I$[d]	14.0[e]	14.0[e]
$C_2H_4I_2\rightarrow C_2H_4+I_2$[d]	0.0[f]	0.0[f]
$C_2H_4I_2\rightarrow C_2H_4+2I$[d]	0.0[f]	0.0[f]
$C_2H_4I+I\rightarrow C_2H_4I-I$[g]	9.3 $(\pm 1.8\times 10^{-1})$[b]	9.2 $(\pm 1.9\times 10^{-1})$[b]
$C_2H_4I\rightarrow C_2H_4+I$[d]	7.4 (± 1.0)[b]	7.6 (± 0.73)[b]
$C_2H_4I-I\rightarrow C_2H_4+I_2$[g]	5.7 (± 0.6)[b]	5.6 (± 0.6)[b]
$I+I\rightarrow I_2$[g]	7.8[h] (± 0.3)	7.8[h] (± 0.3)
Laser spot radius (μm)	37 (± 1.1)[b]	51 (± 13)[b]
Temperature change at 1 μs (K)	1.8	2.1
Density change at 1 μs (kg/m^3)	−2.1	−2.5

[a]Since the initial concentration of $C_2H_4I_2$ is 60 mM, the corresponding concentration is 60 mM × parameter. The fractional concentration of the molecules that are excited and subsequently dissociate into C_2H_4I+I is simply (fractional concentration of excited molecules)–(fractional concentration of rapidly cooled molecules).
[b]The values in parentheses are standard deviation of least-squares fit.
[c]This is simply (fractional concentration of rapidly cooled molecules)/(fractional concentration of excited molecules), not a fitting variable.
[d]The value $10^{\text{parameter}}$ gives the reaction constant in s^{-1}.
[e]This parameter was fixed at this value. Since the time resolution is slower than this process, this parameter did not affect the global fit.
[f]These parameters were fixed at zero since the final values from the global fit were negligible (less than 1×10^{-4}).
[g]The value $10^{\text{parameter}}$ gives the bimolecular reaction constant in mM/s.
[h]This value was fixed at the value according to literature (Ref. 17). The value in the parentheses is the standard deviation when this parameter is included in the global fit.

ACKNOWLEDGMENTS

We are indebted to Fabien Mirloup, Rodolphe Vuillemier, Savo Bratos, and Anton Plech for numerous discussions and advice. We would like to thank Peter Vanderlinden

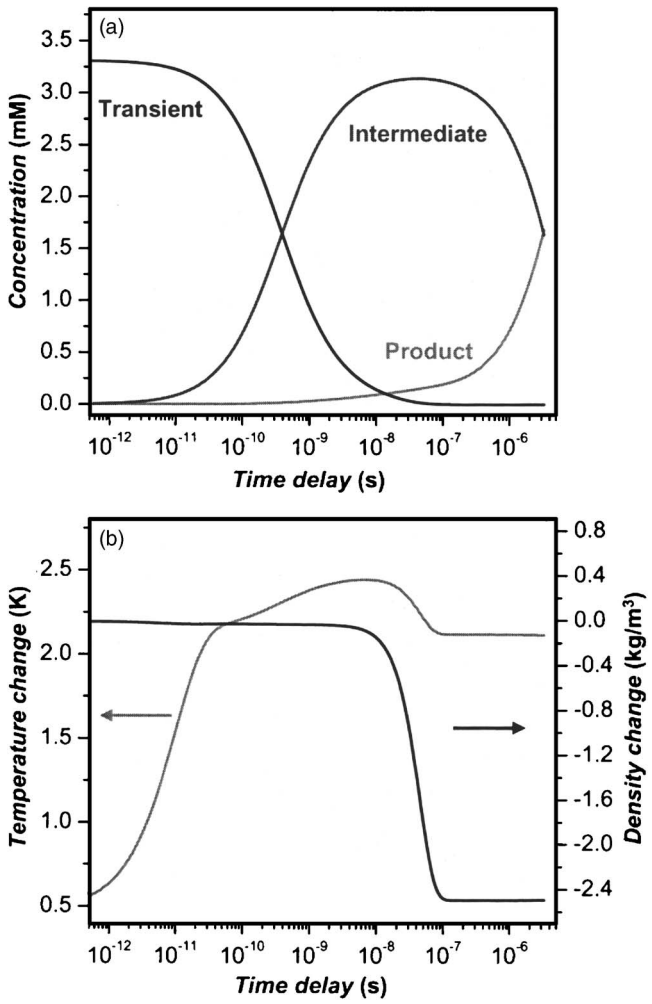

FIG. 7. Time-resolved structural dynamics of the solute and the solvent for $C_2H_4I_2$ in methanol. (A) The population change of the transient C_2H_4I, the intermediate isomer C_2H_4I-I, and the final product I_2 as a function of time delay. (B) The change in the solvent density and the solvent temperature as a function of time delay.

for the extremely efficient design of the temperature controlled cell. This work was supported by the Korea Research Foundation Grant funded by Korean Government (MOE-HRD) (R08-2004-000-10076-0) to HI and by the EU Grant Nos. HPRI-CT-1999-50004 and HPRN-CT-00160.

APPENDIX A: DERIVATION OF THE CORRECTION FORMULA IN EQ. (1)

It is possible to write the following two equations:

$$S_T(q,\rho_{\text{off}}) = N_{\text{off}} S_{\text{sample}}(q,\rho_{\text{off}}) + S_{\text{back}}(q), \tag{A1}$$

$$S_T(q,\rho_{\text{on}}) = \gamma[N_{\text{on}} S_{\text{sample}}(q,\rho_{\text{on}}) + S_{\text{back}}(q)], \tag{A2}$$

where S_T is the total scattering intensity, S_{sample} is the scattering due to the sample alone normalized for the number of molecules (N_{off} and N_{on}) in the x-ray scattering volume, and S_{back} is that due to background of various kinds (air, windows, beam-stop, etc.). This assumption is not trivial since we assume that S_{back} can be measured simply by empting the capillary (in a capillary-based setup) or switching off the liquid jet. The factor γ is to account for the fact that the incoming x-ray flux cannot be assured constant at all times. Denoting q_0 the scattering vector at which we normalize the data and defining

$$\beta = N_{\text{on}}/N_{\text{off}} = 1 + \Delta N/N = 1 + \Delta\rho/\rho \tag{A3}$$

and

$$\alpha = S_{\text{back}}(q_0)/(N_{\text{off}} S_{\text{sample}}(q_0,\rho_{\text{off}})), \tag{A4}$$

we have that the normalization factors (see text) can be written as

$$S_T(q_0,\rho_{\text{off}}) = N_{\text{off}} S_{\text{sample}}(q_0,\rho_{\text{off}}) + \alpha N_{\text{off}} S_{\text{sample}}(q_0,\rho_{\text{off}}), \tag{A5}$$

$$S_T(q_0,\rho_{\text{on}}) = \gamma[N_{\text{on}} S_{\text{sample}}(q_0,\rho_{\text{on}}) + \alpha N_{\text{off}} S_{\text{sample}}(q_0,\rho_{\text{off}})]. \tag{A6}$$

Since q_0 is chosen to be an isobestic point, by definition

$$S_{\text{sample}}(q_0,\rho_{\text{off}}) = S_{\text{sample}}(q_0,\rho_{\text{on}}). \tag{A7}$$

The difference curve obtained by the measurement is defined by $\Delta S_M(q)$,

$$\Delta S_M(q) = S_T(q,\rho_{\text{on}}) \frac{S_T(q_0,\rho_{\text{off}})}{S_T(q_0,\rho_{\text{on}})} - S_T(q,\rho_{\text{off}}). \tag{A8}$$

Inserting previous relations [Eqs. (A1), (A2), and (A5)–(A7)] into Eq. (A8) leads to the following corrected difference curve:

$$\begin{aligned}\Delta S_S(q) &\equiv N_{\text{off}}[S_{\text{sample}}(q,\rho_{\text{on}}) - S_{\text{sample}}(q,\rho_{\text{off}})] \\ &= \frac{1+\alpha/\beta}{1+\alpha}\left\{\Delta S_M(q) + \frac{1-\beta}{\beta+\alpha}[\alpha N_{\text{off}} S_{\text{sample}}(q,\rho_{\text{off}}) - S_{\text{back}}(q)]\right\}.\end{aligned} \tag{A9}$$

We note that the factor γ cancels out in this relation. Typical parameters are $\beta \geqslant 0.997$ (depending on the time delay) and $\alpha \approx 0.5-1.5$.

APPENDIX B: ESTIMATION OF THE DENSITY CHANGE IN EQ. (2)

The energy absorbed by the sample (Q) in the laser illuminated volume V is

$$Q = f N_{\text{abs}} h\nu, \tag{B1}$$

where N_{abs} is the number of molecule that can absorb the pump light, f is the fraction of molecules that have absorbed light, and $h\nu$ is the energy of the pump photon. For time delays shorter than 1 ms it can be shown[10,11] that the energy inside V is conserved. This means that once the pressure is relaxed ($t > 100$ ns) the following relation is valid:

$$Q = N_{\text{solv}} C_p \Delta T, \tag{B2}$$

where N_{solv} is the number of solvent molecule inside V, C_p is the specific heat at constant pressure per molecule, and ΔT the temperature jump. Substituting Eq. (B1) in Eq. (B2) leads to

$$\Delta T = \frac{f N_{\mathrm{abs}} h\nu}{N_{\mathrm{solv}} C_p}. \tag{B3}$$

Moreover, by definition of the expansion coefficient at constant pressure,

$$\alpha_P = \frac{1}{\rho}\left(\frac{\partial \rho}{\partial T}\right)_P, \tag{B4}$$

we have that

$$\frac{\Delta \rho}{\rho} = \alpha_P \Delta T \tag{B5}$$

and finally

$$\frac{\Delta \rho}{\rho} = \alpha_P \Delta T = \alpha_P \frac{f N_{\mathrm{abs}} h\nu}{N_{\mathrm{solv}} C_p}. \tag{B6}$$

For pure solvent measurements, $N_{\mathrm{abs}} = N_{\mathrm{solv}}$. Hence Eq. (B6) simplifies to

$$\frac{\Delta \rho}{\rho} = \alpha_P \frac{f h\nu}{C_p}. \tag{B7}$$

[1] S. Gnanakaran and R. M. Hochstrasser, J. Am. Chem. Soc. **123**, 12886 (2001); S. K. Pal, J. Peon, and A. H. Zewail, Proc. Natl. Acad. Sci. U.S.A. **99**, 1763 (2002).

[2] R. Neutze, R. Wouts, S. Techert, J. Davidsson, M. Kocsis, A. Kirrander, F. Schotte, and M. Wulff, Phys. Rev. Lett. **87**, 195508 (2001).

[3] A. Plech, R. Randler, G. Armin, and M. Wulff, J. Synchrotron Radiat. **9**, 287 (2002); J. Davidsson, J. Poulsen, M. Cammarata *et al.*, Phys. Rev. Lett. **94**, 245503 (2005).

[4] M. Wulff, M. Lorenc, A. Plech, H. Ihee, S. Bratos, F. Mirloup, and R. Vuilleumier, in *Femtochemistry and Femtobiology: Ultrafast Events in Molecular Science*, edited by M. M. Martin and J. T. Hynes (Elsevier, Amsterdam, 2004), p. 337.

[5] A. Plech, M. Wulff, S. Bratos, F. Mirloup, R. Vuilleumier, F. Schotte, and P. A. Anfinrud, Phys. Rev. Lett. **92**, 125505 (2004).

[6] H. Ihee, M. Lorenc, T. K. Kim, Q. Y. Kong, M. Cammarata, J. H. Lee, S. Bratos, and M. Wulff, Science **309**, 1223 (2005).

[7] F. Schotte, S. Techert, P. A. Anfinrud, V. Srajer, K. Moffat, and M. Wulff, in *Third-Generation Hard X-ray Synchrotron Radiation Sources*, edited by D. Mills (Wiley, New York, 2002), p. 345.

[8] A. M. Lindenberg, Y. Acremann, D. P. Lowney, P. A. Heimann, T. K. Allison, T. Matthews, and R. W. Falcone, J. Chem. Phys. **122**, 204507 (2005).

[9] T. S. Dibble and L. S. Bartell, J. Phys. Chem. **96**, 8603 (1992); J. D. Ewbank, J. Y. Luo, J. T. English, R. Liu, W. L. Faust, and L. Schafer, *ibid.* **97**, 8745 (1993); J. C. Williamson, J. Cao, H. Ihee, H. Frey, and A. H. Zewail, Nature (London) **386**, 159 (1997); H. Ihee, J. Cao, and A. H. Zewail, Angew. Chem., Int. Ed. **40**, 1532 (2001); R. C. Dudek and P. M. Weber, J. Phys. Chem. A **105**, 4167 (2001); R. Srinivasan, J. S. Feenstra, S. T. Park, S. J. Xu, and A. H. Zewail, Science **307**, 558 (2005).

[10] S. Bratos, F. Mirloup, R. Vuilleumier, and M. Wulff, J. Chem. Phys. **116**, 10615 (2002).

[11] S. Bratos, F. Mirloup, R. Vuilleumier, and M. Wulff, Chem. Phys. **304**, 245 (2004).

[12] M. Wulff, S. Bratos, A. Plech, R. Vuilleumier, M. Lorenc, Q. Kong, and H. Ihee, J. Chem. Phys. **124**, 034501 (2006).

[13] M. Falk and E. Whalley, J. Chem. Phys. **34**, 1554 (1961).

[14] http://www.esrf.fr/computing/scientific/FIT2D/

[15] P. R. Longaker and M. M. Litvak, J. Appl. Phys. **40**, 4033 (1969).

[16] E. R. Henry and J. Hofrichter, Methods Enzymol. **210**, 129 (1992); H. Ihee, S. Rajagopal, V. Srajer, R. Pahl, S. Anderson, M. Schmidt, F. Schotte, P. A. Anfinrud, M. Wulff, and K. Moffat, Proc. Natl. Acad. Sci. U.S.A. **102**, 7145 (2005).

[17] S. Aditya and J. E. Willard, J. Am. Chem. Soc. **79**, 2680 (1957).